Cooperative Molecular Communication in Drift-Induced Diffusive Cylindrical Channel

Shivani Dhok, *Student Member, IEEE*, Lokendra Chouhan, *Member, IEEE*, Adam Noel, *Member, IEEE*, and Prabhat Kumar Sharma†, *Senior Member, IEEE*

***Abstract*—A cooperative molecular communication (CMC) system is considered inside a cylindrical-shaped channel where a few cooperative nodes (CNs) are intermediately placed between a transmitter (TX) and a fusion center (FC). The expressions for the maximum achievable rate and probability of error at the FC considering AND and OR rules are derived. Furthermore, the performance of the CMC system in a cylindrical channel is compared with the direct and CN-assisted systems. The CMC system with randomly-placed CNs is also analyzed and compared with the uniformly-placed CNs, and it is found that a lower probability of error is obtained in the case of uniform placement of CNs. Furthermore, the system performance as a function of radial displacement of TX and FC under constant flow is compared with that under laminar flow and a higher probability of error is observed under laminar flow. The increased probability of error under laminar flow occurs due to the fact that the drift velocity decreases towards the walls of the cylindrical channel. The analytical expressions are verified using Monte-Carlo simulations.**

***Index Terms*—cooperative nodes, concentration Green's function, fusion center, maximum achievable rate, Molecular communication**

I. Introduction

Molecular communication (MC) systems are inspired by the natural cell-to-cell communication inside organisms, where molecules are used to control the functioning of vital processes, such as signal transduction at the cellular level [1], [2]. In a MC system, the transmitter transmits molecules as the information carriers and the receiver demodulates the information on the basis of some characteristics (e.g., type, release time, number) of the received molecules. For example, protein molecules can function as modulators and demodulators [3]. The biochemical reaction networks at the transmitter modulate the message signal by translating the corresponding inputs into suitable information molecules. The receptors at the receiver are sensitive to the information molecules and are necessary for demodulation. In addition to this, for complex communication systems such as multiple input multiple output (MIMO) and cooperative communication systems, multiple types of proteins could be integrated to implement Boolean logic operations such as AND, OR and XOR [4].

The propagation of molecules in an MC channel can be broadly classified into diffusive and non-diffusive transport methods. The diffusive channel can be further classified into passive and active channels [3]. In passive diffusion, the concentration gradient solely depends on the random propagation of molecules, and can be mathematically modeled by stochastic Brownian motion. In active diffusion, the propagation of molecules depends on both diffusion as well as drift present in the MC channel [5]. Further, the receivers in MC can be classified as active or passive. Active receivers implement chemical reactions to capture and observe molecules. For example, absorbing receivers absorb a fraction of molecules on their surface according to their binding reaction rate, whereas at passive receivers, molecules do not experience any chemical reaction [6]. The receivers can also be classified according to their shapes. The most commonly studied analytical shapes include point and spherical receivers [7].

In MC, the peak molecule concentration may degrade strongly with distance during propagation between transmitter (TX) and receiver (RX) [8]. Moreover, the molecules may undergo a degradation reaction leading to the formation of a different type of molecule that cannot be identified by the receiver. In addition, the outer boundaries of the environment may be absorbing or reflective [9], and the former type will lead to a reduction in the number of molecules reaching the receiver in a confined environment. Thus, long distance transmission of molecules can be impractical, even if the channel includes a drift towards the receiver. To achieve longer distance MC, relay-assisted and cooperative communication systems have been recently explored. In relay-assisted systems, the cooperative nodes (CNs) assist the TX for transmission of information to the RX when direct communication between TX and RX is not possible. There are several existing works in the available literature that have focused on cooperative and relay-assisted MC systems [10]–[13]. In [10], the initial study of the relay-assisted system, two scenarios for sensing and forwarding of information from transmitter to receiver with the assistance of a relay were proposed. In [11], a decode-and-forward relaying method was proposed for communication between two populations of biological agents. The authors

This work was an outcome of the R&D work undertaken in the project under the Visvesvaraya PhD Scheme of Ministry of Electronics Information Technology, Government of India, being implemented by Digital India Corporation (formerly Media Lab Asia).

Shivani Dhok is with Department of ECE, Indian Institute of Information Technology, Nagpur, India (e-mail: shivanid17499@gmail.com). She contributed to this work as a part of her project under supervision of Dr. Prabhat Kumar Sharma.

Lokendra Chouhan is with the Department of Electrical Engineering, Indian Institute of Technology, Indore, India (e-mail: lokendrachouhan22@gmail.com).

Adam Noel is with the School of Engineering (Systems and Information Stream) at the University of Warwick, Coventry, UK, CV4 7AL (email: adam.noel@warwick.ac.uk)

Prabhat Kumar Sharma is with the Department of ECE, Visvesvaraya National Institute of Technology, Nagpur, India (e-mail: prabhatmadhavec1@gmail.com).

†Corresponding Author

of [12] extended dual-hop MC to any number of hops. [13] considered a cooperative MC arrangement where signals were combined at a Fusion Center (FC) and the system performance was analyzed in terms of average error probability using hard decision rules. Work in [14] analyzed the performance of dual-hop and multi-hop MC systems in terms of average probability of error and information rate.

The early detection of diseases and particulate drug delivery inside organisms using invasive techniques are potential applications of MC, where a group of transmitters and receivers collectively identify the disease by coordinating and communicating among each other and delivering medication to a diseased area [15]. There are several existing works [15]–[18] that have proposed application-specific MC system models for 1-D and 3-D channels. For example, cooperative abnormality detection where several sensors are used to identify malignancy in a three-dimensional unbounded environment was presented in [15]. In [17], abnormality detection in a one-dimensional channel was proposed. Early detection of cancerous cells using mobile nanosensors (MNS) was considered in [18]. All these works have used either a 1-D or unbounded 3-D structure as a communication channel. However, many practical scenarios, e.g., blood vessels, are both 3-D and bounded, which merits dedicated consideration.

Several works [9], [19]–[24] have modelled the communication inside bounded environments. For example, a bounded diffusion-based MC system with a partially absorbing receiver was described in [19]. Particle propagation inside a diffusive cylindrical MC channel with vertical force was proposed in [20]. Another example of diffusion-dominated motion in a cylindrical model was presented in [21], where a ring-shaped receiver with Poiseuille flow was considered. The software platform BiNS2 was presented in [22] for visualization of diffusion-based MC in a drift-induced channel. In [23], a cylindrical vessel with non-uniform drift was considered. An experimental setup for MC inside a cylinder was presented in [24], where a pH-based modulation technique was applied. In [9] the Green's function for the concentration profile of molecules inside a cylindrical environment was analyzed and the performance for a single source and sink was derived. All the aforementioned works using bounded communication channels [9], [19]–[24] have considered only a direct link between a transmitter and receiver. However, as we discussed, direct communication between transmitter and receiver may be impractical, so it is worthwhile to consider cooperative molecular communication (CMC) for these bounded systems. To the best of our knowledge, CMC in *bounded* systems is an open problem that has not been addressed in the existing literature. Motivated by these ideas, the key contributions of this paper are as follows:

1) We consider a drift-induced diffusive cooperative communication arrangement inside blood-vessel-like MC channels approximated as cylinders.
2) The expressions for average probability of error are derived at an FC considering AND and OR fusion rules.
3) For the considered system model, expressions for mutual information and maximum achievable rate are derived incorporating AND and OR rules.

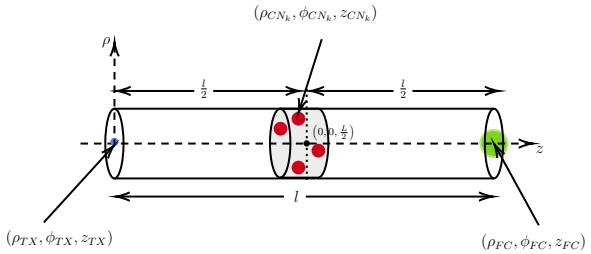

Fig. 1: Schematic of the considered cylindrical 3-D model, where the blue point denotes the TX, and red and green circles denote the CNs and FC, respectively.

4) The performance of the CMC system is compared with the direct-path and the CN-assisted path in terms of the average probability of error.
5) The effect of different system parameters such as channel radius, drift, diffusion coefficient, the position of TX, FC and CNs, and the degradation constant are considered. We also compare the system performance for laminar and constant flow as well as for uniformly-placed and randomly-placed CNs.

All of the analytical results are verified using Monte-Carlo simulations.

The rest of this paper is organized as follows. Section II describes the transmission channel model. The analytical expressions for the proposed model and the equations for the maximum achievable rate are derived in Section III and Section IV, respectively. The numerical and simulation results are discussed in Section V. Finally, the conclusions are drawn in Section VI.

II. Transmission Channel Model

Fig. 1 shows a schematic representation of the considered MC system. The transmission channel is modelled as a semi-infinite three-dimensional cylindrical vessel structure with $0 \leq \rho < \rho_c$, $0 \leq \phi \leq 2\pi$ and $0 \leq z < \infty$, where ρ_c is the radius of the vessel. We assume a constant drift of fluid medium along the $z-$direction, $v = v_z \widehat{a}_z$ ms^{-1}, where v_z and $\widehat{a}_z$ are the magnitude of velocity and unit vector along the $z-$axis, respectively. All emitted molecules undergo irreversible degradation with rate α s^{-1}. Moreover, we consider a purely reflective boundary, indicating no absorption of molecules at the walls. A single-transmitter single-fusion center model is adopted, where we consider a point TX positioned at $(\rho_{\text{TX}}, \phi_{\text{TX}}, z_{\text{TX}})$ and a spherical passive FC of radius R_{FC} at location $(\rho_{\text{FC}}, \phi_{\text{FC}}, z_{\text{FC}})$, such that the axial distance between the TX and the center of the FC is l. We consider K number of spherical passive CNs placed uniformly along the azimuthal axis around the axial center $(0, 0, \frac{l}{2})$ between the TX and FC with constant radial distance. Moreover, the axial position of the CNs is considering the fact that the lowest error probability is achieved at the center position [25]. The position of the kth CN is denoted by $(\rho_{\text{CN},k}, \phi_{\text{CN},k}, z_{\text{CN},k})$, where $k \in \{1, 2, 3, \ldots, K\}$. The radius of all the CNs is considered to be equal to R_{CN}. Similar to [9], we assume that

the TX, FC, and CNs are anchored to fixed locations using rigid supports suspended from the vessel wall.

The TX can release a maximum number N_A of molecules of type A in one impulsive release with uniform diffusion coefficient D_A m^2/s. The information transmission from TX is a binary sequence of length L denoted by $\mathrm{X}^L = \{x[1], x[2], \ldots, x[L]\}$, where $x[j] \in \{0, 1\}$ denotes the bit transmission in the jth time-slot and $j \in \{1, 2, 3, \ldots, L\}$. For modulation, on-off-keying (OOK) is used at the TX. In OOK, TX transmits $x[j] = 1$ by releasing N_A molecules and no molecules are transmitted for $x[j] = 0$. Prior probabilities for the transmissions of $x[j] = 1$ and $x[j] = 0$ are represented by β_1 and β_0, respectively. Moreover, we consider a full-duplex decode-and-forward (DF) relaying transmission scheme, i.e., CNs can transmit and receive information in the same time-slot [11], [25], [26]. In DF relaying, the symbol transmitted from the TX is first decoded at each CN and later the decoded symbol is transmitted to the FC using OOK. The FC makes an individual decision depending on the molecules received from each CN. We let the decoded binary sequence at the kth CN be represented as $\widehat{\mathrm{X}}_k^L = \{\widehat{x}_k[1], \widehat{x}_k[2], \ldots, \widehat{x}_k[L]\}$, and the decoded binary sequence at the FC corresponding to the kth CN be denoted as $\mathrm{Y}_k^{L+1} = \{y_k[2], y_k[3], \ldots, y_k[L+1]\}$. We assume that the TX and each CN emit different types of molecules to limit the effect of self-interference, i.e., the TX emits N_A number of molecules of type A and the kth CN emits $N_{B,k}$ number of molecules with diffusion coefficient D_B[1]. Moreover, we assume that the FC has receptors that can detect the K different types of molecules emitted by the CNs. At long transmission distances ($\approx 60\mu$m), the number of molecules observed at the FC that were transmitted by the TX is very low in comparison to the number of molecules received from the CNs, and those molecules have a longer propagation time, so we ignore them at the FC. The details for the same can be found in Secion-V.

In order to ascertain the number of molecules arriving at a CN or the FC, we then first determine the concentration profile of the molecules. For analyzing the concentration profile we use the concentration Green's function ($C(\rho, \phi, z, t|\rho_o, \phi_o, z_o, t_o)$) subjected to Robin's boundary condition given by (1) listed at the top of the following page [9, eq. 29]. J_n and γ_{nm} in (1) are the nth order Bessel function of the first kind and the eigenvalues, respectively. $u(t)$ is the Heaviside function. We define U_n and W_{nm} as

$$U_n = \begin{cases} \frac{1}{2\pi} & \text{if } n = 0, \\ \frac{1}{\pi} & \text{if } n \geq 1, \end{cases} \tag{2}$$

$$W_{nm} = \frac{\rho_c^2}{2}(J_n^2(\gamma_{nm}\rho_c) - J_{n-1}(\gamma_{nm}\rho_c)J_{n+1}(\gamma_{nm}\rho_c)). \tag{3}$$

Molecule releases by TX and CN are considered to be impulsive releases given by $s(\rho, \phi, z, t|\rho_o, \phi_o, z_o) = \frac{\delta(\rho-\rho_o)}{\rho}\delta(\phi - \phi_o)\delta(z - z_o)$, where $\delta(\cdot)$ is the Dirac delta function and (ρ_o, ϕ_o, z_o) is the location of the releasing entity. For spherical CNs, we assume this location is the center of the CN. The probability that a released molecule is observed in a spherical region covering the set of points V at time t is given by [9, eq. 32] as

$$p(t) = \int\int\int_V C(\rho, \phi, z, t|\rho_o, \phi_o, z_o, t_o)\rho d\rho d\phi dz, \tag{4}$$

where t_o is the initial time instant. Considering a spherical region of very small radius R_v, (4) can be approximated as

$$p(t) = \frac{4}{3}\pi R_v^3 C(\rho, \phi, z, t|\rho_o, \phi_o, z_o, t_o). \tag{5}$$

We let T_p be the transmission duration for one bit. The jth time-slot is $[(j-1)T_P, jT_p]$ and the probability of observing the molecules at the end of this time-slot is given by $p_0(T_p)$, where 0 in the subscript indicates the current time-slot. Considering the inter symbol interference (ISI), the molecules released in the previous ith time-slot ($[(i-1)T_p, iT_p]$), where $i \in \{1, 2, 3, \ldots j-1\}$, would be interfering with the molecules in the current time-slot. The probability that molecules released in the ith slot are received in the jth slot is given by,

$$p_{j-i} = \frac{4}{3}\pi R_v^3 C(\rho, \phi, z, (j-i)T_p|\rho_o, \phi_o, z_o, t_o), \tag{6}$$

and here $i = j$ corresponds to the current time-slot.

III. Probability of Error Analysis

We consider the CNs to be operating independently and the local decisions by each CN are independent of the decisions of the other CNs. This local decision by CN is communicated to the FC. The FC, considering all the local decisions received from the CNs, generates a final global decision. As the CNs are passive, the molecules neither undergo any chemical reactions that are unique to the CNs within CNs' boundaries, nor are absorbed. Hence, we assume that each molecule is available to be sensed by each CN, and each CN can count the number of molecules within its boundary, without affecting the molecules' characteristics. Moreover, we assume the CNs to be capable of making independent observations. The number of molecules received at the kth CN in the jth time-slot ($N_{\mathrm{CN},k}[j]$) is defined as follows,

$$N_{\mathrm{CN},k}[j] = N^C_{\mathrm{CN},k}[j] + N^I_{\mathrm{CN},k}[j] + N^o_{\mathrm{CN},k}[j],$$

where $N^C_{\mathrm{CN},k}[j]$ are the molecules received due to transmission in the jth time-slot, $N^I_{\mathrm{CN},k}[j]$ denotes the ISI due to the transmissions in previous time-slots and $N^o_{\mathrm{CN},k}[j]$ is multiple source interference (MSI), which may occur due to molecules arriving from secondary sources. The number of molecules received in the jth time-slot, that were transmitted in the ith time-slot is a Binomial random variable (RV). For a large number of transmitted molecules and a small arrival probability the Binomial distribution can be approximated as a Poisson distribution [28]. The total number of molecules received from all time-slots, which is a summation of Poisson RVs, is therefore also a Poisson RV [28]. Therefore,

$$N^C_{\mathrm{CN},k}[j] \sim \mathcal{P}\left(N_A p_0 x[j]\right) = \mathcal{P}\left(\lambda^C_{\mathrm{CN},k}\right),$$

$$N^I_{\mathrm{CN},k}[j] \sim \mathcal{P}\left(N_A \sum_{i=1}^{j-1} p_i x[j-i]\right) = \mathcal{P}\left(\lambda^I_{\mathrm{CN},k}\right),$$

[1]Natural MC transmitters such as eukaryotic cells can be genetically modified to emit different types of molecules [27] for transmission.

$$C(\rho,\phi,z,t|\rho_o,\phi_o,z_o,t_o) = \frac{1}{\sqrt{4\pi D(t-t_o)}} e^{\frac{-(z-z_o-v(t-t_o))}{4D(t-t_o)} - \alpha(t-t_o)} \sum_{n=0}^{\infty}\sum_{m=1}^{\infty} \frac{U_n J_n(\gamma_{nm}\rho_o)}{W_{nm}} J_n(\gamma_{nm}\rho)\cos(n(\phi-\phi_o)) e^{-D\gamma_{nm}^2(t-t_o)} u(t-t_o), \quad (1)$$

and $N^o_{\text{CN},k}[j] \sim \mathcal{P}\left(\lambda^o_{\text{CN},k}\right)$,

where p_i denotes the probability of arrival from the $(j-i)$th previous time-slot and is obtained by evaluating (6) at $(\rho_o,\phi_o,z_o) = (\rho_{\text{TX}},\phi_{\text{TX}},z_{\text{TX}})$, $(\rho,\phi,z) = (\rho_{\text{CN},k},\phi_{\text{CN},k},z_{\text{CN},k})$, and $R_v = R_{\text{CN}}$.

From the property of summation of independent variables, the total number of molecules received at the kth CN in the intended jth time-slot also follows a Poisson distribution with mean parameters

$$\lambda_{\text{CN},k}[j] = \lambda^C_{\text{CN},k}[j] + \lambda^I_{\text{CN},k}[j] + \lambda^o_{\text{CN},k}[j], \quad (7)$$

where $\lambda^C_{\text{CN},k}[j]$, $\lambda^I_{\text{CN},k}[j]$, and $\lambda^o_{\text{CN},k}[j]$ are the mean number of intended molecules received in the jth time slot, ISI, and MSI, respectively. Hence, the total number of molecules received at the kth CN in the jth time-slot is given by two hypotheses,

$$\begin{aligned}\mathcal{H}_0^{\text{CN},k} : N_{\text{CN},k}[j] &\sim \mathcal{P}\left(\lambda^I_{\text{CN},k}[j] + \lambda^o_{\text{CN},k}[j]\right) \\ &= \mathcal{P}\left(\lambda^0_{\text{CN},k}[j]\right), \quad (8)\\ \mathcal{H}_1^{\text{CN},k} : N_{\text{CN},k}[j] &\sim \mathcal{P}\left(\lambda^C_{\text{CN},k}[j] + \lambda^I_{\text{CN},k}[j] + \lambda^o_{\text{CN},k}[j]\right) \\ &= \mathcal{P}\left(\lambda^1_{\text{CN},k}[j]\right), \quad (9)\end{aligned}$$

where $\lambda^0_{\text{CN},k}[j] = \lambda^I_{\text{CN},k}[j] + \lambda^o_{\text{CN},k}[j]$ and $\lambda^1_{\text{CN},k}[j] = \lambda^C_{\text{CN},k}[j] + \lambda^I_{\text{CN},k}[j] + \lambda^o_{\text{CN},k}[j]$ denote the expected number of molecules corresponding to the symbols 0 and 1, respectively.

Depending on the value of $N_{\text{CN},k}[j]$, the local decision rule at the kth CN for the symbol $\widehat{x}_k[j]$ corresponding to the decision threshold $\widehat{\eta}[j]$ is defined as

$$\widehat{x}_k[j] = \begin{cases} 1 & \text{if } N_{\text{CN},k}[j] > \widehat{\eta}[j], \\ 0 & \text{otherwise.} \end{cases} \quad (10)$$

Based on the independent local decisions, each CN releases $N_{B,k}$ number of molecules to indicate the transmission of bit '1'. The number of molecules received at the FC due to the kth CN is denoted by $N_{\text{FC},k}[j+1]$, such that

$$N_{\text{FC},k}[j+1] = N^C_{\text{FC},k}[j+1] + N^I_{\text{FC},k}[j+1] + N^o_{\text{FC},k}[j+1],$$

where $N^C_{\text{FC},k}[j+1]$, $N^I_{\text{FC},k}[j+1]$ and $N^o_{\text{FC},k}[j+1]$ are the number of intended molecules received in the $(j+1)$th slot, ISI, and MSI, respectively, and can also be approximated with a Poisson RV as

$$\begin{aligned}N^C_{\text{FC},k}[j+1] &\sim \mathcal{P}\left(N_{B,k} p_0^{\text{FC},k}\right) \\ &= \mathcal{P}\left(\lambda^C_{\text{FC},k}[j+1]\right),\end{aligned}$$

$$\begin{aligned}N^I_{\text{FC},k}[j+1] &\sim \mathcal{P}\left(N_{B,k}\sum_{i=2}^{j-1} p_i^{\text{FC},k}\widehat{x}[j-i+2]\right) \\ &= \mathcal{P}\left(\lambda^I_{\text{FC},k}[j+1]\right), \\ N^o_{\text{FC},k}[j+1] &\sim \mathcal{P}\left(\lambda^o_{\text{FC},k}[j+1]\right).\end{aligned}$$

The number of molecules received at the FC in the intended time-slot, defined using two hypotheses, is given as,

$$\begin{aligned}\mathcal{H}_0^{\text{FC},k} : N_{\text{FC},k}[j+1] &\sim \mathcal{P}\left(\lambda^0_{\text{FC},k}[j+1]\right), \\ \mathcal{H}_1^{\text{FC},k} : N_{\text{FC},k}[j+1] &\sim \mathcal{P}\left(\lambda^1_{\text{FC},k}[j+1]\right), \quad (11)\end{aligned}$$

where $\lambda^0_{\text{FC},k} = \lambda^I_{\text{FC},k}[j] + \lambda^o_{\text{FC},k}[j]$ and $\lambda^1_{\text{FC},k} = \lambda^C_{\text{FC},k}[j] + \lambda^I_{\text{FC},k}[j] + \lambda^o_{\text{FC},k}[j]$. At the FC, the signals received from all the CNs are treated independently and finally, the global decision is determined by evaluating decisions from each CN. Let $y_k[j+1]$ be the symbol generated corresponding to the number of molecules received from the kth CN in the $(j+1)$th time-slot, such that

$$y_k[j+1] = \begin{cases} 1 & \text{if } N_{\text{FC},k}[j+1] > \eta[j+1], \\ 0 & \text{otherwise,} \end{cases} \quad (12)$$

where $\eta[j+1]$ is the decision threshold at the FC. For the possible combinations of sequences of previous bits $\left(\text{X}^{j-1}\right)$ at the TX, the error in the final decision at the FC depends on the errors that may occur in the K individual CN-assisted links. For the kth link, an error could occur if either $x[j] \neq \widehat{x}_k[j]$ and $\widehat{x}_k[j] = y_k[j+1]$ or $x[j] = \widehat{x}_k[j]$ and $\widehat{x}_k[j] \neq y_k[j+1]$.

In order to determine the performance analysis, we use two different decision rules: AND and OR rules. Before individually analyzing each rule, we derive local detection and false alarm probabilities at the kth CN as well as for the FC. The probabilities of false alarm and detection at the kth CN due to transmission from TX in the jth time slot are given as

$$\begin{aligned}P^{\text{fa}}{}_{\text{CN},k}\left[j|\text{X}^{j-1}\right] &= \Pr\left[\widehat{x}_k[j] = 1 | x[j] = 0, \text{X}^{j-1}\right] \\ &= \Pr\left(N_{\text{CN},k}[j] > \widehat{\eta}[j] | x[j] = 0, \text{X}^{j-1}\right) \\ &= 1 - \Pr\left(N_{\text{CN},k}[j] \leq \widehat{\eta}[j] | x[j] = 0, \text{X}^{j-1}\right) \\ &= 1 - \sum_{l=1}^{\widehat{\eta}[j]} \frac{e^{-\lambda^0_{\text{CN},k}[j]}\left(\lambda^0_{\text{CN},k}[j]\right)^l}{l!}, \quad (13)\end{aligned}$$

$$\begin{aligned}P^{\text{d}}{}_{\text{CN},k}\left[j|\text{X}^{j-1}\right] &= \Pr\left[\widehat{x}_k[j] = 1 | x[j] = 1, \text{X}^{j-1}\right] \\ &= \Pr\left[N_{\text{CN},k}[j] > \widehat{\eta}[j] | x[j] = 1, \text{X}^{j-1}\right] \\ &= 1 - \sum_{l=1}^{\widehat{\eta[j]}} \frac{e^{-\lambda^1_{\text{CN},k}[j]}\left(\lambda^1_{\text{CN},k}[j]\right)^l}{l!}. \quad (14)\end{aligned}$$

The detection and false alarm probabilities at the FC due to the transmission from the kth CN in the $(j+1)$th time-slot

and possible combinations $\left(\widehat{\mathrm{X}}_k^{j-1}\right)$ at the kth CN are given as

$$\begin{aligned} &P^{\text{fa}}{}_{\text{FC},k}\left[j+1|\widehat{\mathrm{X}}_k^{j-1}\right] \\ &= \Pr\left(y_k[j+1]=1|\widehat{x}_k[j+1]=0,\widehat{\mathrm{X}}_k^{j-1}\right) \\ &= \Pr\left(N_{\text{FC},k}[j+1]>\eta[j+1]|\widehat{x}_k[j+1]=0,\widehat{\mathrm{X}}_k^{j-1}\right) \\ &= 1-\Pr\left(N_{\text{FC},k}[j+1]\leq\eta[j+1]\ |\widehat{x}_k[j+1]=0,\widehat{\mathrm{X}}_k^{j-1}\right) \\ &= 1-\sum_{l=1}^{\eta[j+1]}\frac{e^{-\lambda^0_{\text{FC},k}[j+1]}\left(\lambda^0_{\text{FC},k}[j+1]\right)^l}{l!}, \end{aligned} \tag{15}$$

and,

$$\begin{aligned} &P^{\text{d}}{}_{\text{FC},k}[j+1|\widehat{\mathrm{X}}_k^{j-1}] \\ &= \Pr\left(y_k[j+1]=1|\widehat{x}_k[j]=1,\widehat{\mathrm{X}}_k^{j-1}\right) \\ &= \Pr\left(N_{\text{FC},k}[j+1]>\eta[j+1]|\widehat{x}_k[j]=1,\widehat{\mathrm{X}}_k^{j-1}\right) \\ &= 1-\sum_{l=1}^{\eta}\frac{e^{-\lambda^1_{\text{FC},k}[j+1]}\left(\lambda^1_{\text{FC},k}[j+1]\right)^l}{l!}, \end{aligned} \tag{16}$$

where $\lambda^0_{\text{FC},k}[j+1]=\lambda^I_{\text{FC},k}[j+1]+\lambda^o_{\text{FC},k}[j+1]$ and $\lambda^1_{\text{FC},k}[j+1]=\lambda^C_{\text{FC},k}[j+1]+\lambda^I_{\text{FC},k}[j+1]+\lambda^o_{\text{FC},k}[j+1]$.

For the global decision at FC, we employ AND and OR rules, which are the extreme cases of the *m-out-of-k* hard decision rule [29]. The AND rule corresponds to the condition of $m=k$, whereas OR rule corresponds to $m=1$ [29]. The hard decision rules enable the combining of the local binary decoded decisions at the FC, instead of making decisions directly based on the energy or the number of molecules [30]. We note that the hard decision rules have been proven to be energy efficient [31]. Several MC research works have used the hard decision rules for global decision estimation at the FC [13], [17], [29], [32].

A. AND Rule

AND rule is the hard decision rule that generates a global decision as '1' if all the CNs report '1' as their information bits. In order to define the global error probability, we define the global probability of detection $\left(Q^{\text{d}}_{\text{AND}}[j+1|\mathrm{X}^{j-1}]\right)$ as [17]

$$\begin{aligned} Q^{\text{d}}_{\text{AND}}\left[j+1|\mathrm{X}_1^{j-1}\right] &= \Pr\left(y[j+1]=1|x[j]=1,\mathrm{X}^{j-1}\right) \\ &= \prod_{k=1}^{K}\Pr\left(y_k[j+1]=1|x[j]=1,\mathrm{X}^{j-1}\right). \end{aligned} \tag{17}$$

Similarly, the probability of false alarm $\left(Q^{\text{fa}}_{\text{AND}}[j+1|\mathrm{X}^{j-1}]\right)$ is given as

$$\begin{aligned} Q^{\text{fa}}_{\text{AND}}\left[j+1|\mathrm{X}_1^{j-1}\right] &= \Pr\left(y[j]=1|x[j]=0,\mathrm{X}^{j-1}\right) \\ &= \prod_{k=1}^{K}\Pr\left(y_k[j+1]=1|x[j]=0,\mathrm{X}^{j-1}\right), \end{aligned} \tag{18}$$

where $\Pr\left(y_k[j+1]=1|x[j]=1,\mathrm{X}^{j-1}\right)$ and $\Pr\left(y_k[j+1]=1|x[j]=0,\mathrm{X}^{j-1}\right)$ are obtained in (19) and (20), respectively, at the top of the next page.

Finally, we define the probability of error as

$$\begin{aligned} P^e_{\text{AND}}\left[j+1|\mathrm{X}^{j-1}\right] &= \beta_0\times Q^{\text{fa}}_{\text{AND}}[j+1|\mathrm{X}^{j-1}] \\ &\quad+\beta_1\times(1-Q^{\text{d}}_{\text{AND}}[j+1|\mathrm{X}^{j-1}]). \end{aligned} \tag{21}$$

The end-to-end average probability of error in the $(j+1)$th time-slot, $\overline{P}^e_{\text{AND}}[j+1]$, is calculated by averaging $P^e_{\text{AND}}\left[j+1|\mathrm{X}^{j-1}\right]$ over all the possible realizations of X^{j-1}, i.e,

$$\overline{P}^e_{\text{AND}}[j+1]=\sum_{\mathrm{X}^{j-1}\in\chi}\Pr\left(\mathrm{X}^{j-1}\right)P^e_{\text{AND}}\left[j+1|\mathrm{X}^{j-1}\right], \tag{22}$$

where χ is the set of all possible realizations of X^{j-1}, and $\Pr\left(\mathrm{X}^{j-1}\right)$ is the probability of occurrence of X^{j-1}.

B. OR Rule

We define hard decision OR rule which leads to a global decision as '1' if at least one CN reports '1' as their information bit. Similar to AND rule, we define the probability of detection $Q^{\text{d}}_{\text{OR}}\left[j+1|\mathrm{X}^{j-1}\right]$ as

$$Q^{\text{d}}_{\text{OR}}\left[j+1|\mathrm{X}^{j-1}\right]=1-\prod_{k=1}^{K}\Pr\left(y_k[j+1]=0|x[j]=1,\mathrm{X}^{j-1}\right). \tag{23}$$

Similarly, the probability of false alarm $\left(Q^{\text{fa}}_{\text{OR}}\left[j+1|\mathrm{X}^{j-1}\right]\right)$ is given as

$$Q^{\text{fa}}_{\text{OR}}\left[j+1|\mathrm{X}_1^{j-1}\right]=1-\prod_{k=1}^{K}\Pr\left(y_k[j+1]=0|x[j]=0,\mathrm{X}^{j-1}\right), \tag{24}$$

where $\Pr\left(y_k[j+1]=0|x[j]=1,\mathrm{X}^{j-1}\right)$ and $\Pr\left(y_k[j+1]=0|x[j]=0,\mathrm{X}^{j-1}\right)$ are determined in (25) and (26), respectively, at the top of the next page.

Hence, the error probability is defined as

$$\begin{aligned} P^e_{\text{OR}}\left[j+1|\mathrm{X}^{j-1}\right] &= \beta_0\times Q^{\text{fa}}_{\text{OR}}\left[j+1|\mathrm{X}^{j-1}\right] \\ &\quad+\beta_1\times\left(1-Q^{\text{d}}_{\text{OR}}\left[j+1|\mathrm{X}^{j-1}\right]\right). \end{aligned} \tag{27}$$

Now, the end-to-end average probability of error in the $(j+1)$th time-slot, $\overline{P}^e_{\text{OR}}[j+1]$, is calculated by averaging $P^e_{\text{OR}}\left[j+1|\mathrm{X}^{j-1}\right]$ over all the possible realizations of X^{j-1} i.e.,

$$\overline{P}^e_{\text{OR}}[j+1]=\sum_{\mathrm{X}^{j-1}\in\chi}\Pr\left(\mathrm{X}^{j-1}\right)P^e_{\text{OR}}\left[j+1|\mathrm{X}^{j-1}\right], \tag{28}$$

where χ is a set of all the possible realizations of X^{j-1}, and $\Pr\left(\mathrm{X}^{j-1}\right)$ is the probability of occurrence of X^{j-1}.

IV. Maximum Achievable Rate

In this section, we derive the entropy-based expression for maximum achievable rate considering the AND and OR rules for the cooperative channel. If $\mathrm{X}[j]$ and $\mathrm{Y}[j+1]$ are two discrete RVs indicating the transmitted and received symbols in the jth and $(j+1)$th time-slots, respectively, then the mutual information $I(\mathrm{X}[j];\mathrm{Y}[j+1])$ is given by [33, Ch. 9]

$$\begin{aligned}\Pr\left(y_k[j+1]=1 \mid x[j]=1,\mathrm{X}^{j-1}\right) &= \Pr\left(y_k[j+1]=1 \mid \widehat{x}_k[j]=1,\widehat{\mathrm{X}}_k^{j-1}\right)\times \Pr\left(\widehat{x}_k[j]=1 \mid x[j]=1,\mathrm{X}^{j-1}\right)\\ &+ \Pr\left(y_k[j+1]=1 \mid \widehat{x}_k[j]=0,\widehat{\mathrm{X}}_k^{j-1}\right)\times \Pr\left(\widehat{x}_k[j]=\ 0 \mid x[j]=1,\mathrm{X}^{j-1}\right)\\ &= P^{\mathrm{d}}_{\mathrm{FC},k}\left[j+1 \mid \widehat{\mathrm{X}}_k^{j-1}\right]\times P^{\mathrm{d}}_{\mathrm{CN},k}\left[j \mid \mathrm{X}^{j-1}\right]+P^{\mathrm{fa}}_{\mathrm{FC},k}\left[j+1 \mid \widehat{\mathrm{X}}_k^{j-1}\right]\times\left(1-P^{\mathrm{d}}_{\mathrm{CN},k}\left[j \mid \mathrm{X}^{j-1}\right]\right) \quad (19)\\ \Pr\left(y_k[j+1]=1 \mid x[j]=0,\mathrm{X}^{j-1}\right) &= \Pr\left(y_k[j+1]=1 \mid \widehat{x}_k[j]=1,\widehat{\mathrm{X}}_k^{j-1}\right)\times \Pr\left(\widehat{x}_k[j]=1 \mid x[j]=0,\mathrm{X}^{j-1}\right)\\ &+ \Pr\left(y_k[j+1]=1 \mid \widehat{x}_k[j]=0,\widehat{\mathrm{X}}_k^{j-1}\right)\times \Pr\left(\widehat{x}_k[j]=\ 0 \mid x[j]=0,\mathrm{X}^{j-1}\right)\\ &= P^{\mathrm{d}}_{\mathrm{FC},k}\left[j+1 \mid \widehat{\mathrm{X}}_k^{j-1}\right]\times P^{\mathrm{fa}}_{\mathrm{CN},k}\left[j \mid \mathrm{X}^{j-1}\right]+P^{\mathrm{fa}}_{\mathrm{FC},k}\left[j+1 \mid \widehat{\mathrm{X}}_k^{j-1}\right]\times\left(1-P^{\mathrm{fa}}_{\mathrm{CN},k}\left[j \mid \mathrm{X}^{j-1}\right]\right) \quad (20)\end{aligned}$$

$$\begin{aligned}\Pr\left(y_k[j+1]=0 \mid x[j]=1,\mathrm{X}^{j-1}\right) &= \Pr\left(y_k[j+1]=0 \mid \widehat{x}_k[j]=1,\widehat{\mathrm{X}}_k^{j-1}\right)\times \Pr\left(\widehat{x}_k[j]=1 \mid x[j]=1,\mathrm{X}^{j-1}\right)\\ &+ \Pr\left(y_k[j+1]=0 \mid \widehat{x}_k[j]=0,\widehat{\mathrm{X}}_k^{j-1}\right)\times \Pr\left(\widehat{x}_k[j]=0 \mid x[j]=1,\mathrm{X}^{j-1}\right)\\ &= \left(1-P^{\mathrm{d}}_{\mathrm{FC},k}\left[j+1 \mid \widehat{\mathrm{X}}_k^{j-1}\right]\right)\times P^{\mathrm{d}}_{\mathrm{CN},k}\left[j \mid \mathrm{X}^{j-1}\right]+\left(1-P^{\mathrm{fa}}_{\mathrm{FC},k}\left[j+1 \mid \widehat{\mathrm{X}}_k^{j-1}\right]\right)\times\left(1-P^{\mathrm{fa}}_{\mathrm{CN},k}\left[j \mid \mathrm{X}^{j-1}\right]\right) \quad (25)\\ \Pr\left(y_k[j+1]=0 \mid x[j]=0,\mathrm{X}^{j-1}\right) &= \Pr\left(y_k[j+1]=\ 0 \mid \widehat{x}_k[j]=1,\widehat{\mathrm{X}}_k^{j-1}\right)\times \Pr\left(\widehat{x}_k[j]=1 \mid x[j]=0,\mathrm{X}^{j-1}\right)\\ &+ \Pr\left(y_k[j+1]=0 \mid \widehat{x}_k[j]=0,\widehat{\mathrm{X}}_k^{j-1}\right)\times \Pr\left(\widehat{x}_k[j]=0 \mid x[j]=0,\mathrm{X}^{j-1}\right)\\ &= \left(1-P^{\mathrm{d}}_{\mathrm{FC},k}\left[j+1 \mid \widehat{\mathrm{X}}_k^{j-1}\right]\right)\times P^{\mathrm{fa}}_{\mathrm{CN},k}\left[j \mid \mathrm{X}^{j-1}\right]+\left(1-P^{\mathrm{fa}}_{\mathrm{FC},k}\left[j+1 \mid \widehat{\mathrm{X}}_k^{j-1}\right]\right)\times\left(1-P^{\mathrm{fa}}_{\mathrm{CN},k}\left[j \mid \mathrm{X}^{j-1}\right]\right) \quad (26)\end{aligned}$$

$$I\left(\mathrm{X}[j];\mathrm{Y}[j+1]\right)=H(Y[j+1])-H(Y[j+1]|X[j])\,, \quad (29)$$

where the entropy of $Y[j+1]$, $H(Y[j+1])$ is given as

$$H\left(Y[j+1]\right)=-\sum_{y[j+1]\in\{0,1\}}\Pr\left(y[j+1]\right)\log_2\left(\Pr\left(y[j+1]\right)\right) \quad (30)$$

such that

$$\begin{aligned}\Pr\left(y[j+1]=1\right) &= \beta_0\Pr\left(y[j+1]=1|\,x[j]=0\right)\\ &+ \beta_1\Pr\left(y[j+1]=1|x[j]=1\right)\\ &= \beta_0 p_{10}+\beta_1 p_{11}, \quad (31)\\ \Pr\left(y[j+1]=0\right) &= \beta_0\Pr\left(y[j+1]=0|x[j]=0\right)\\ &+ \beta_1\Pr\left(y[j+1]=0|x[j]=1\right)\\ &= \beta_0 p_{00}+\beta_1 p_{01}. \quad (32)\end{aligned}$$

The value of conditional entropy $H(Y[j+1]|X[j])$ is given as

$$\begin{aligned}H(Y[j+1]|X[j]) &= -\sum_{x[j]\in\{0,1\}}\Big(\Pr(x[j])\\ &\sum_{y[j+1]\in\{0,1\}}\Pr\left(y[j+1]|x[j]\right)\log_2\left(\Pr\left(y[j+1]|x[j]\right)\right)\Big) \quad (33)\\ &= -\beta_0\left(p_{00}\log_2\left(p_{00}\right)+p_{10}\log_2\left(p_{10}\right)\right)\\ &\quad -\beta_1\left(p_{10}\log_2\left(p_{10}\right)+p_{11}\log_2\left(p_{11}\right)\right), \quad (34)\end{aligned}$$

where the conditional probabilities, $\Pr(y[j+1]|x[j])$, are given as

$$\begin{aligned}p_{00} &= \Pr(y[j+1]=0|x[j]=0)\\ &= \Pr(y[j+1]=0|\widehat{x}[j]=0)\times\Pr(\widehat{x}[j]=0|x[j]=0)\\ &+ \Pr(y[j+1]=0|\widehat{x}[j]=1)\times\Pr(\widehat{x}[j]=1|x[j]=0)\\ p_{00} &= \begin{cases}1-Q^{\mathrm{fa}}_{\mathrm{AND}}\left[j+1|\mathrm{X}_1^{j-1}\right] & \text{(AND Rule)}\\ 1-Q^{\mathrm{fa}}_{\mathrm{OR}}\left[j+1|\mathrm{X}_1^{j-1}\right] & \text{(OR Rule),}\end{cases} \quad (35)\end{aligned}$$

$$\begin{aligned}p_{01} &= \Pr(y[j+1]=0|x[j]=1)\\ &= \Pr(y[j+1]=0|\widehat{x}[j]=0)\times\Pr(\widehat{x}[j]=0|x[j]=1)\\ &+ \Pr(y[j+1]=0|\widehat{x}[j]=1)\times\Pr(\widehat{x}[j]=1|x[j]=1)\\ p_{01} &= \begin{cases}1-Q^{\mathrm{d}}_{\mathrm{AND}}\left[j+1|\mathrm{X}_1^{j-1}\right] & \text{(AND Rule)}\\ 1-Q^{\mathrm{d}}_{\mathrm{OR}}\left[j+1|\mathrm{X}_1^{j-1}\right] & \text{(OR Rule),}\end{cases} \quad (36)\end{aligned}$$

$$\begin{aligned}p_{10} &= \Pr(y[j+1]=1|x[j]=0)\\ &= \Pr(y[j+1]=1|\widehat{x}[j]=0)\times\Pr(\widehat{x}[j]=0|x[j]=0)\\ &+ \Pr(y[j+1]=1|\widehat{x}[j]=1)\times\Pr(\widehat{x}[j]=1|x[j]=0)\\ p_{10} &= \begin{cases}Q^{\mathrm{fa}}_{\mathrm{AND}}\left[j+1|\mathrm{X}_1^{j-1}\right] & \text{(AND Rule)}\\ Q^{\mathrm{fa}}_{\mathrm{OR}}\left[j+1|\mathrm{X}_1^{j-1}\right] & \text{(OR Rule),}\end{cases} \quad (37)\end{aligned}$$

$$\begin{aligned}p_{11} &= \Pr(y[j+1]=1|x[j]=1)\\ &= \Pr(y[j+1]=1|\widehat{x}[j]=0)\times\Pr(\widehat{x}[j]=0|x[j]=1)\\ &+ \Pr(y[j+1]=1|\widehat{x}[j]=1)\times\Pr(\widehat{x}[j]=1|x[j]=1)\\ p_{11} &= \begin{cases}Q^{\mathrm{d}}_{\mathrm{AND}}\left[j+1|\mathrm{X}_1^{j-1}\right] & \text{(AND Rule)}\\ Q^{\mathrm{d}}_{\mathrm{OR}}\left[j+1|\mathrm{X}_1^{j-1}\right] & \text{(OR Rule).}\end{cases} \quad (38)\end{aligned}$$

Now, the maximum achievable rate can be obtained by maximizing the mutual information as

$$C_s=\max_{\beta_1}\left\{I(\mathrm{X}[j];\mathrm{Y}[j+1])\right\} \quad \text{bits/slot.} \quad (39)$$

TABLE I: System parameters.

Parameter	Description	Value
ρ_c	Radius of blood vessel	5 μm
$D = D_A = D_B$	Diffusion coefficient	10^{-9} m^2/s
$(\rho_{\text{TX}}, \phi_{\text{TX}}, z_{\text{TX}})$	TX position	(0,0,0)
R_{RX} and R_{CN}	RX and CN radius	1 μm
R_{FC}	FC radius	1 μm
$N_A + N_{B,k}$	Maximum number of molecules transmitted for direct-path, CN-assisted, and CMC systems	50000
α	Degradation constant	9 s^{-1}
	Number of Time Slots for ISI	5
l	Distance between TX and FC or RX	60 μm
$(\rho_{\text{FC}}, \phi_{\text{FC}}, z_{\text{FC}})$	FC position	$(0, 0, 60\ \mu\text{m})$
v	Drift velocity	60 μm/s
K	Number of CNs	3

V. Simulation and Numerical Results

We use Monte-Carlo simulations with 10^3 realizations to assess the validity of the derived expressions as well as to analyze the system performance. The main equation that governs the molecules' movement due to diffusion and drift is (1), which was first introduced in [9]. The authors of [9] validated the equation in their work using particle-based simulations. Hence, it is not necessary to re-validate the expression and we can rely on the more efficient Monte-Carlo simulation approach for analyzing the channel performance at the FC. We assume the position of TX as $(0, 0, 0)$ and that of FC as $(0, 0, 60)$ μm. We consider $K = 3$ cooperative nodes that are located at an axial distance of $\frac{l}{2} = 30$ μm, displaced radially by $\rho_{CN,k} = 2$ μm and at an angular separation of 120°. In other words, the placement of CNs is uniform along the circumference of a circle of radius $\rho_{CN,k}$ and fixed at the axial center between TX and FC to obtain minimum probability of error. The parameters v, D and ρ_c are chosen to give a nominal Peclet number[2] equal to 0.6, which indicates that the diffusive transport is somewhat greater than the drift. The value of symbol duration T_p is determined on the basis of peak concentration, i.e., T_p is chosen to be the time corresponding to the peak concentration for the diffusion wave from the TX to the CNs. The simulation parameters are considered as shown in Table I unless specified otherwise.

A comparison for the probability of error for the case of uniformly-placed CNs and non-uniformly-placed CNs is shown in Fig. 2. The non-uniform placement is such that the CNs are randomly placed (without overlapping) in a cylindrical region of height 4 μm and radius 4 μm, which is centered at the axial center of the cylindrical channel. We observe that the performance degrades if the CNs are randomly placed instead of uniform placement. This is due to the fact that, in non-uniform placement, CNs may be positioned in such a way that the distance from TX to CN$_k$, or CN$_k$ to FC increases, leading to a reduction in molecule hitting probability at CN or FC. Considering these facts, the uniform placement of CNs is preferred for the rest of the analysis.

We compare the performance of the direct-path, CN-assisted and CMC models in Fig. 3. The direct-path system is the case

[2]Peclet number [34, ch. 9], $P_{ne} = \frac{2\rho_c \times v}{D}$ and for the considered channel the value of $P_{ne} = \frac{2\times5\times10^{-6}\times60\times10^{-6}}{10^{-9}} = 0.6$.

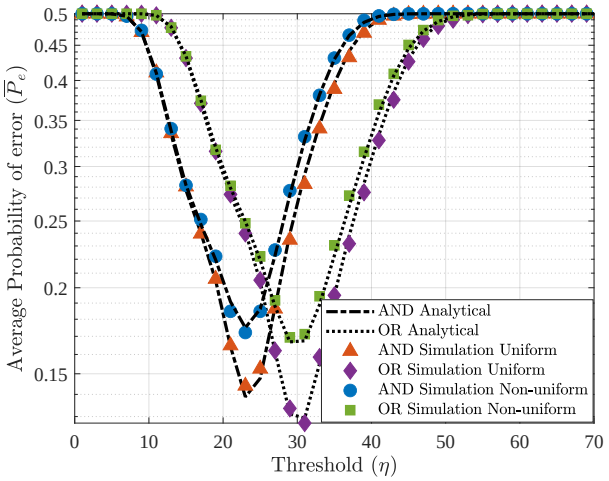

Fig. 2: The comparison for uniform and non-uniform placement of the CNs, for $K = 3$.

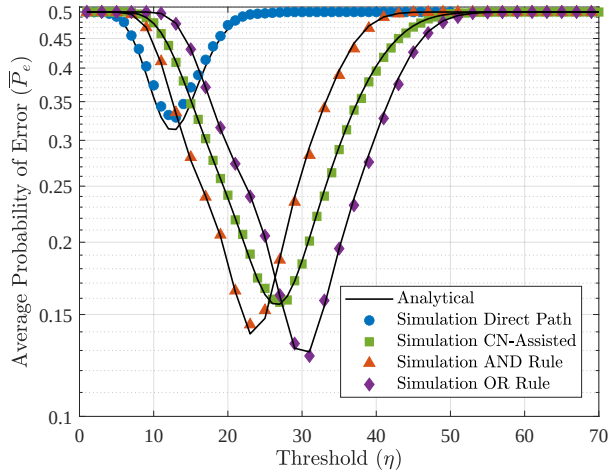

Fig. 3: Comparision of $\overline{P}_e$ of direct-path, CN-assisted and CMC systems as a function of decision threshold η.

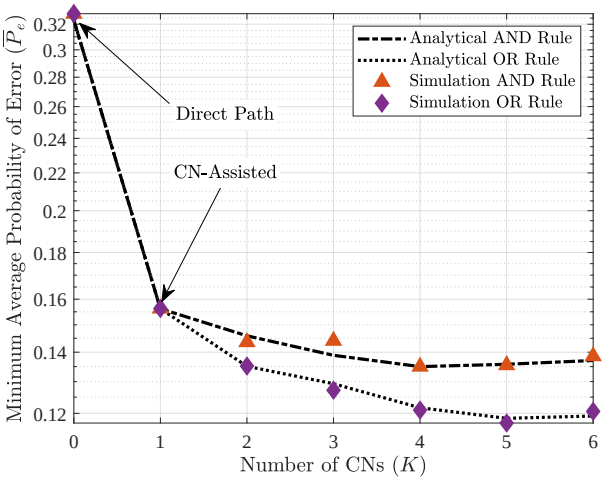

Fig. 4: Effect of number of CNs on the minimum average probability of error (i.e., with the optimal decision threshold).

when there is no assistance from any relay, and the CN-assisted system is the case when the transmission is assisted by a single relaying node, i.e., when $K = 1$. Note that, for the CN-assisted case, the CN is placed directly on the axis between the TX and FC $(0, 0, 30\ \mu\text{m})$, whereas in CMC, the CNs are displaced radially at a distance of 2 μm from the axis. We consider the number of molecules transmitted over a transmission-path, $\text{TX} - \text{CN}_k - \text{FC}$ (or for direct-path, $\text{TX} - \text{FC}$) as a constant of 5×10^4. We recall that, at long distance transmissions, for CN-assisted and CMC systems, the effect of molecules transmitted by TX and observed at FC is not considered. We observe that, at a distance of 60 μm and drift velocity of 60 μm/s, the number of molecules released by the TX and arriving at the FC is around 2, such that the arrival probability is on the order of 10^{-5}, whereas the number of molecules received from each CN is around 25 with arrival probability of the order of 10^{-3}. Considering these facts, we ignore the effect of the molecules transmitted by the TX at the FC. From Fig. 3, we observe that the CMC system has a lower average probability of error in comparison to the direct-path and CN-assisted system.

Fig. 4 shows the performance of $\overline{P}_e$ as a function of the number of CNs. We note that the optimum value of the threshold is found using numerical methods with the help of the MATLAB function `fminunc()`, which uses a quasi-Newton algorithm to obtain the threshold corresponding to the minimum average probability of error. From this figure, it can be concluded that the performance of the system improves as the number of CNs increases. This is because, for a larger number of CNs, the detection probability at the FC increases, whereas the probability of false alarm at FC decreases. We note that the maximum number of CNs is restricted by the bounded environment. The maximum number of CNs (K) can be determined using $2\pi\rho_{CN,k} > 2R_{CN}K$. Hence, the maximum value of K for the considered set of parameters with no overlaps of the CNs is $K = 6$. We also note that the minimum $\overline{P}_e$ is lower for OR rule compared to AND rule for $K > 1$. We recall that $K = 0$ and $K = 1$ indicate the direct-path and CN-assisted scenarios, respectively. As the number of reporting nodes at the FC is one in both of these cases, there is no requirement to apply any decision rule. The OR rule can detect the received bit as '1' if at least one of the CNs report '1'. This leads to a lower probability of error for OR rule when compared to AND rule for less reliable transmissions, e.g., over longer distances. Moreover, the degree of performance improvement is less for the AND rule in comparison to that for the OR rule.

Various system parameters (e.g., radius of channel, drift velocity, degradation constant, distance between the TX and FC) also affect the system performance. First, we analyze the effect of the radius of the channel (ρ_c) on the minimum $\overline{P}_e$ in Fig. 5. In this figure, we observe that performance degrades for higher values of radius ρ_c. This is due to the fact that when the radius increases, molecules can diffuse radially over a longer distance, so some of the molecules may not be detected by the CN or FC.

We analyze the effect of the degradation coefficient α in Fig. 6. We observed that the value of $\overline{P}_e$ initially decreases to its lowest value around 7 s^{-1} and further increases with α for both

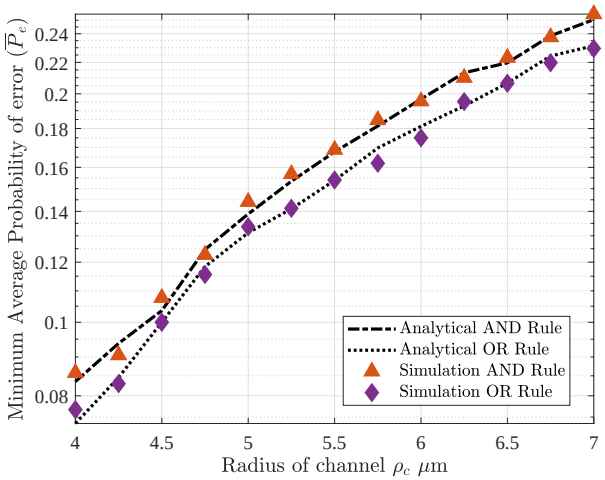

Fig. 5: Effect of radius of the channel (ρ_c) on minimum average probability of error.

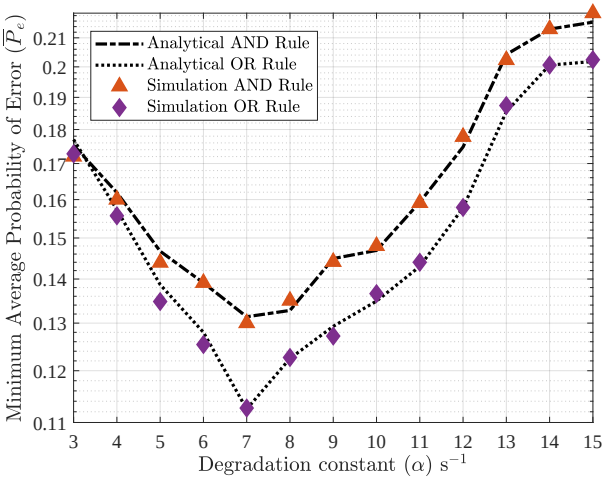

Fig. 6: Effect of degradation constant on minimum average probability of error.

AND and OR rules. This is because for lower values of α, i.e., at $\alpha = 7\ \text{s}^{-1}$, the degradation of the intended molecules at the CNs and the FC is offset by the degradation of ISI molecules, whereas for higher values of α, i.e., at $\alpha > 7\ \text{s}^{-1}$, the reduction in ISI is offset by the degradation of the molecules intended for the current time slot.

Moreover, we analyze the effect of the drift velocity v in Fig. 7. In Fig. 7(a), $\overline{P}_e$ is plotted as a function of decision threshold. we can observe from this figure that a lower value of $\overline{P}_e$ is achieved for $v = 60$ μm/s in comparison to the case for $v = 30$ μm/s. It is observed from Fig. 7(b) that, as v increases from 30 μm/s to 70 μm/s, the minimum $\overline{P}_e$ decreases, thereby improving the system performance. This is because a higher drift value leads to a higher arrival probability of molecules at CNs and at the FC. Furthermore, the combined effect of v and diffusion coefficient D is analyzed in Fig. 8. It is observed that for constant v, the minimum $\overline{P}_e$ is lower for $D = 0.5 \times 10^{-9}$ followed by $D = 1 \times 10^{-9}$ m^2/s and $D = 1.5 \times 10^{-9}$ m^2/s for

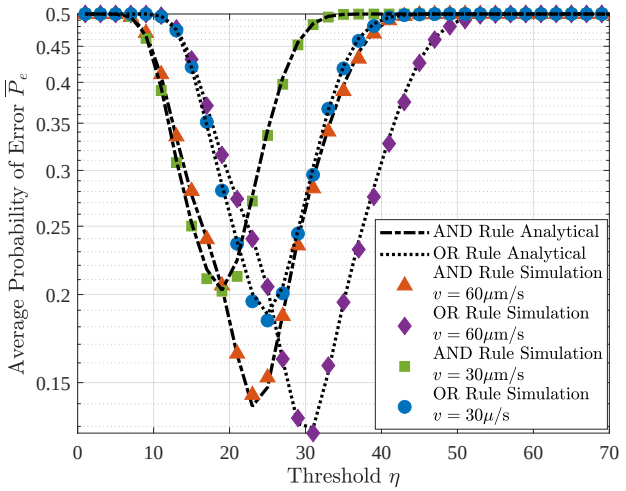

(a) $\overline{P}_e$ vs η

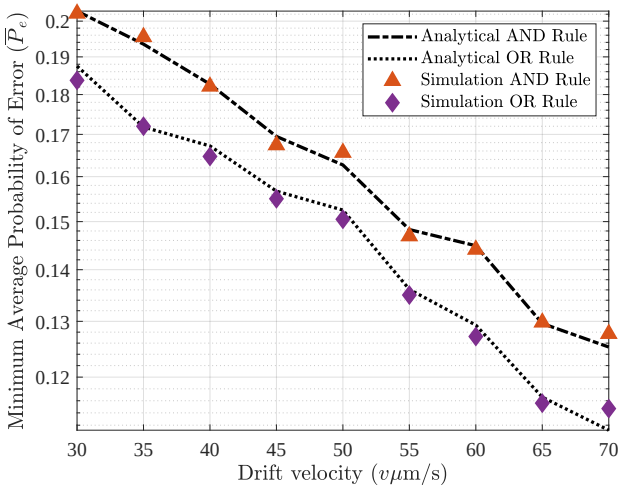

(b) Minimum $\overline{P}_e$ vs v

Fig. 7: (a) Average probability of error as a function of decision threshold. (b) Minimum average probability of error as a function of drift velocity.

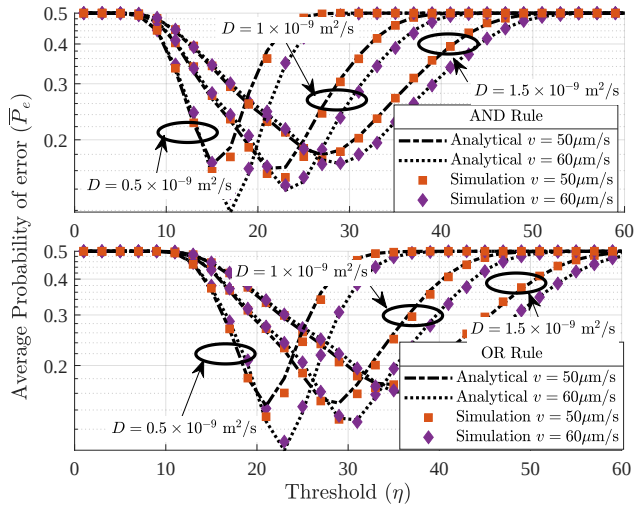

Fig. 8: Effect of drift velocity (v) and diffusion coefficient (D) on the average probability of error.

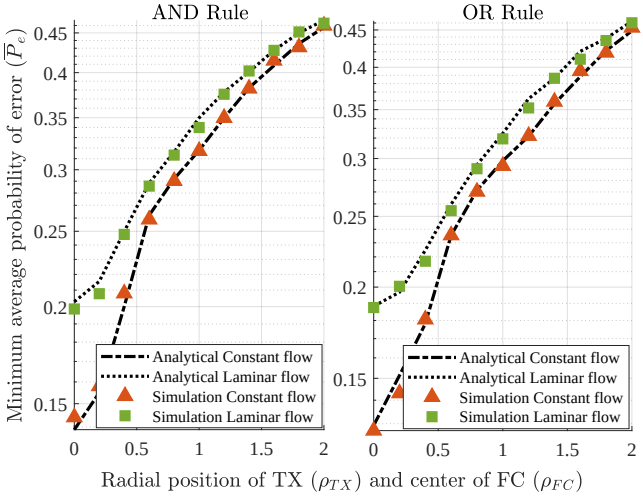

Fig. 9: Comparison of $\overline{P}_e$ for laminar and constant flow.

both AND and OR rules. Furthermore, we also see that $\overline{P}_e$ is lower for high values of v when keeping D fixed, which is consistent with the observations in Fig. 7.

We compare the performance for constant drift and laminar flow as a function of radial displacement (with constant axial and azimuthal coordinates) of the TX and FC in Fig. 9. The laminar flow at radial distance ρ for the cylindrical channel of radius ρ_c is given as $v(\rho) = 2v_{\text{eff}}\left(1 - \frac{\rho^2}{\rho_c^2}\right)$ [35], [36]. The laminar flow can be investigated in two regimes, namely dispersion or diffusion regime $(v_{\text{eff}}\rho_c/D \ll 4l/\rho_c)$ and flow-dominated regime $(v_{\text{eff}}\rho_c/D \gg 4l/\rho_c)$. In the diffusion or dispersion regime, the laminar flow can be approximated as a uniform flow with effective diffusion coefficient $D_{\text{eff}} = D\left(1 + \frac{1}{48}\left(\frac{v_{\text{eff}}\rho_c}{D}\right)^2\right)$, where $v_{\text{eff}} = \frac{v_{\max}}{2}$ is the average velocity of the laminar flow [35]. We note that the maximum velocity of the laminar flow is observed at the center of the channel, i.e. at $\rho = 0$ where $v = v_{\max}$. For a fair comparison, we keep the value of $v_{\max}$ for laminar flow and the value of constant velocity to 60 μm/s, by setting a common upper-limit on the maximum possible velocity that can be observed inside the channel. It can be observed from the figure that the performance degrades for laminar flow. This is as a result of reduced velocity towards the cylindrical surface boundary. Furthermore, we can observe that, if we displace TX and FC radially, the performance degrades with an increase in the radial distance.

Fig. 10 shows the mutual information as a function of prior probability (β_1) and decision threshold (η). The peak values of $I(X[j]; Y[j+1])$ for a given decision threshold gives the maximum achievable rate. Interestingly, we also observe that the maximum achievable rate shows a bimodal behavior for fixed β_1 as a function of decision threshold. This

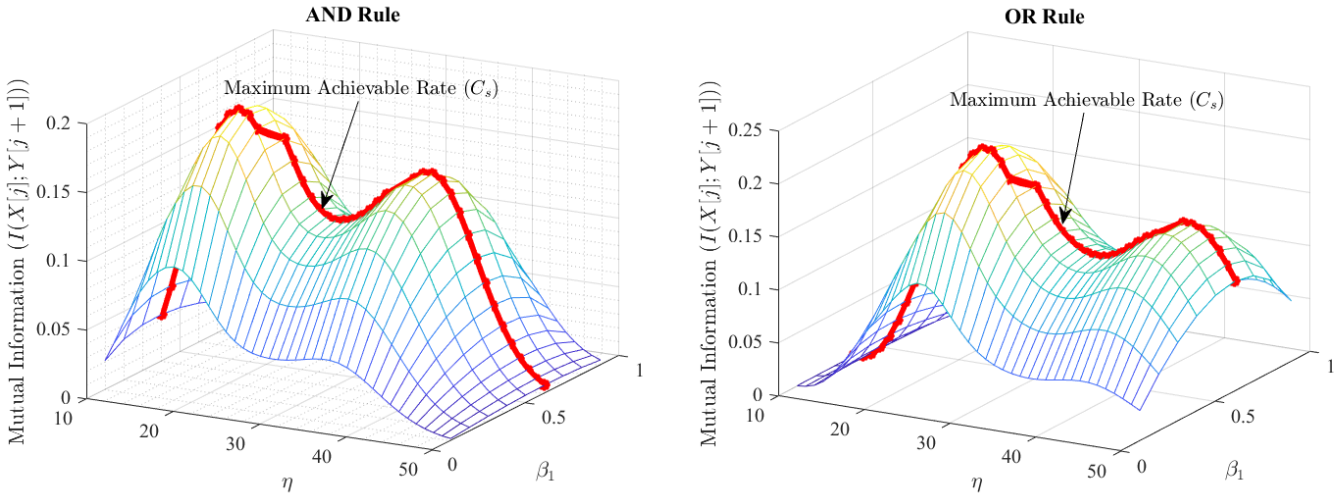

(a) $I(X[j];Y[j+1])$ vs β_1 and η (b) $I(X[j];Y[j+1])$ vs β_1 and η

Fig. 10: (a) Mutual information as function of prior probability (β_1) and decision threshold (η) in case of AND rule for. (b) Mutual information as function of prior probability (β_1) and decision threshold (η) in case of OR rule.

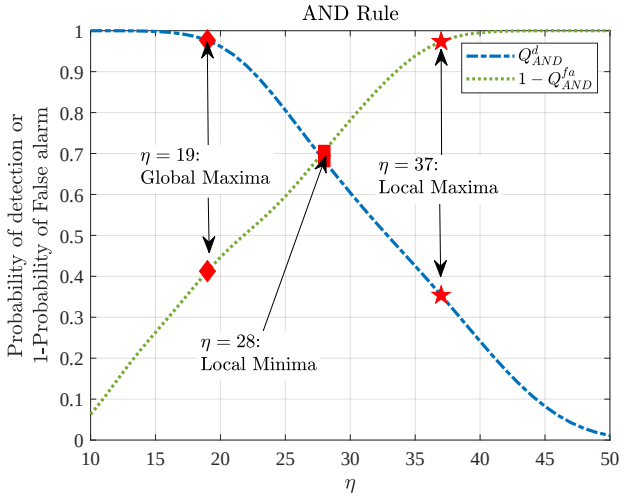

Fig. 11: Probability of detection $\left(Q^{\text{d}}_{\text{AND}}\right)$ and complement of probability of false alarm $\left(1-Q^{\text{fa}}_{\text{AND}}\right)$ vs η for AND rule.

is because of the complementary performance of false alarm and detection, as shown in Fig. 11 for AND rule (similar observations can be made for OR rule). For low decision threshold (up to the first peak, i.e., global maximum), the maximum achievable rate is dominated by the high probability of false alarm whereas the probability of detection is nearly fixed. As the decision threshold increases enough for the probability of detection to degrade, the maximum achievable rate decreases to a local minimum. However, for even higher decision thresholds the probability of false alarm becomes very low and a local maximum in achievable rate is observed. Beyond this point, the maximum achievable rate is dominated by the poor probability of detection.

The performance of the system for varying distance between the TX and FC is analyzed using the maximum achievable rate in Fig. 12(a). The maximum achievable rate is plotted as a function of threshold in Fig. 12(a). From this figure, we observe that the OR rule outperforms the AND rule for maximum achievable rate. The higher value of maximum achievable rate for OR rule cannot be guaranteed for all values of η due to the bimodal nature of the maximum achievable rate and mutual information. Moreover from this figure, we also observe that the maximum achievable rate is higher at a distance of 60 μm than at a distance of 70 μm. A similar trend is observed when the maximum achievable rate is plotted as a function of the distance between the TX and FC. It is evident from Fig. 12(b) that the peak maximum achievable rate decreases as the distance between TX and FC increases. This is consistent with the deterioration in channel performance and is as expected, since a larger distance between the TX and FC leads to a reduction in the molecule reception probability at FC. Moreover, the OR rule achieves a higher peak maximum achievable rate as it requires only one CN reporting '1'.

VI. Conclusion

In this paper, we considered an active cooperative molecular communication (CMC) system inside a semi-infinite length tubular structure. For CMC, we considered CNs that respond to the symbols received from the TX by transmitting local decisions to the fusion center (FC). At the FC, local decisions from the independent CNs are interpreted and the global decision is found by combining the reported decisions and applying the AND and OR decision rules. We assumed an On-Off Keying (OOK) modulation scheme for transmission of bits. The expressions for the average probability of error and maximum achievable rate for the CMC system were derived and the performance was compared with the direct-path and CN-assisted models. We observed that cooperative communication outperformed the direct-path and CN-assisted models even at comparatively larger distances. Variations in the channel performance due to changes in the system parameters were assessed. Initially, the performance for uniformly-

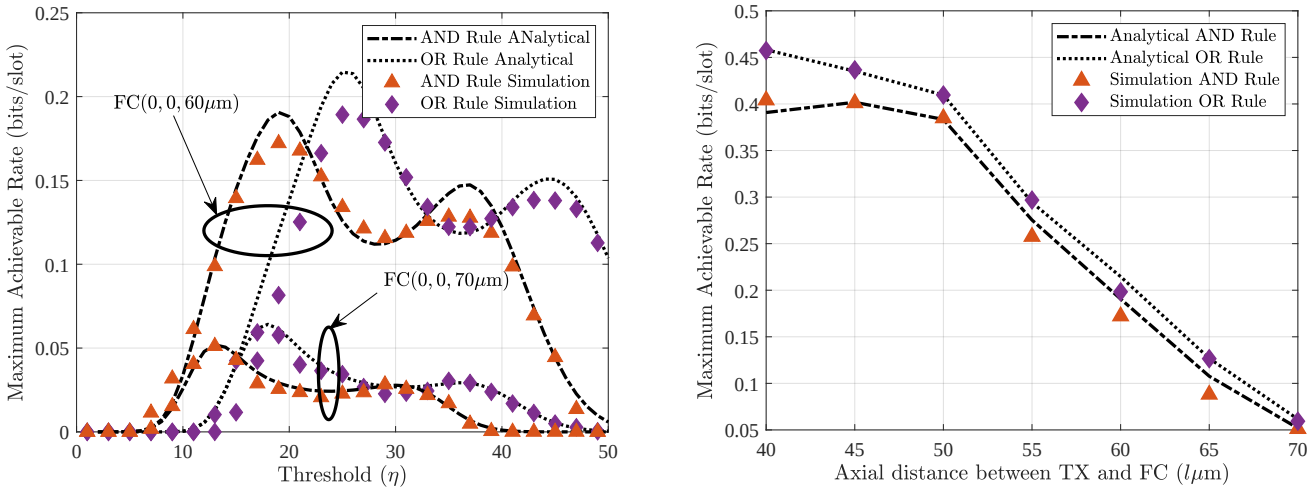

(a) C_s vs η (b) C_s vs l

Fig. 12: (a) Maximum achievable rate as a function of threshold for different values of distance between TX and FC. (b) Maximum achievable rate versus axial distance between TX and FC.

placed and non-uniformly placed CNs were compared and we observed deteriorated performance for non-uniform placement when compared to the uniform placement of CNs. We also observed that as the radius of the cylindrical channel increases, the performance of the system deteriorates. Furthermore, we observed that the performance improved with an increase in drift velocity and the number of CNs, whereas it deteriorated with an increase in distance between the TX and FC and diffusion coefficient. The effect of laminar flow and radial displacement of the TX and FC was also analyzed and we observed that the average probability of error increased if laminar flow is considered. It was also observed that, with an increase in radial displacement of TX and FC, the probability of error increases for both laminar and constant flow. In case of increasing degradation constant, the performance improved to an optimal point and then deteriorated as too many signalling molecules were destroyed. The proposed MC model could be extended for anomaly detection inside blood vessels by introducing non-uniformity in some of the system parameters such as the diffusion coefficient.

REFERENCES

[1] C. M. Waters and B. L. Bassler, "Quorum sensing: cell-to-cell communication in bacteria," *Annual Review of Cell and Developmental Biology*, vol. 21, pp. 319–346, Nov. 2005.

[2] B. L. Bassler, "Small talk: cell-to-cell communication in bacteria," *Cell*, vol. 109, pp. 421 – 424, May 2002.

[3] T. Nakano, A. Eckford, and T. Haraguchi, *Molecular Communication*. Molecular Communication, Cambridge University Press, 2013.

[4] E. Katz and V. Privman, "Enzyme-based logic systems for information processing," *Chemical Society Reviews*, vol. 39, pp. 1835–1857, Mar. 2010.

[5] K. V. Srinivas, A. W. Eckford, and R. S. Adve, "Molecular communication in fluid media: The additive inverse gaussian noise channel," *IEEE Trans. on Info. Theory*, vol. 58, pp. 4678–4692, Jul. 2012.

[6] A. Einolghozati, M. Sardari, and F. Fekri, "Capacity of diffusion-based molecular communication with ligand receptors," in *Proc. 2011 IEEE Info. Th. Workshop*, pp. 85–89, Oct. 2011.

[7] N. Farsad, H. B. Yilmaz, A. Eckford, C. Chae, and W. Guo, "A comprehensive survey of recent advancements in molecular communication," *IEEE Commun. Sur. Tuto.*, vol. 18, pp. 1887–1919, 3rd quarter 2016.

[8] Y. Murin, N. Farsad, M. Chowdhury, and A. Goldsmith, "Communication over diffusion-based molecular timing channels," in *Proc. 2016 IEEE Global Commun. Conf. (GLOBECOM)*, pp. 1–6, Dec. 2016.

[9] M. Zoofaghari and H. Arjmandi, "Diffusive molecular communication in biological cylindrical environment," *IEEE Trans. NanoBio.*, vol. 18, pp. 74–83, Jan. 2019.

[10] A. Einolghozati, M. Sardari, and F. Fekri, "Relaying in diffusion-based molecular communication," in *Proc. 2013 IEEE Int. Symp. on Info. Theo.*, pp. 1844–1848, Jul. 2013.

[11] A. Einolghozati, M. Sardari, and F. Fekri, "Decode and forward relaying in diffusion-based molecular communication between two populations of biological agents," in *Proc. 2014 IEEE Int. Conf. on Commun. (ICC)*, pp. 3975–3980, Jun. 2014.

[12] A. Ahmadzadeh, A. Noel, and R. Schober, "Analysis and design of multi-hop diffusion-based molecular communication networks," *IEEE Trans. on Mol., Bio. and Multi-Scale Commun.*, vol. 1, pp. 144–157, Jun. 2015.

[13] Y. Fang, A. Noel, N. Yang, A. W. Eckford, and R. A. Kennedy, "Convex optimization of distributed cooperative detection in multi-receiver molecular communication," *IEEE Trans. on Mol., Bio. and Multi-Scale Commun.*, vol. 3, pp. 166–182, Sep. 2017.

[14] N. Varshney, A. Patel, A. K. Jagannatham, and P. K. Varshney, "Design and performance analysis of dual and multi-hop diffusive molecular communication systems," *CoRR*, vol. abs/1710.00555, Oct. 2017.

[15] R. Mosayebi, V. Jamali, N. Ghoroghchian, R. Schober, M. Nasiri-Kenari, and M. Mehrabi, "Cooperative abnormality detection via diffusive molecular communications," *IEEE Trans. on NanoBio.*, vol. 16, pp. 828–842, Dec. 2017.

[16] S. Ghavami and F. Lahouti, "Abnormality detection in correlated gaussian molecular nano-networks: Design and analysis," *IEEE Trans. on NanoBio.*, vol. 16, pp. 189–202, Apr. 2017.

[17] N. Varshney, A. Patel, Y. Deng, W. Haselmayr, P. K. Varshney, and A. Nallanathan, "Abnormality detection inside blood vessels with mobile nanomachines," *IEEE Trans. on Mol., Bio. and Multi-Scale Commun.*, vol. 4, pp. 189–194, Sep. 2018.

[18] R. Mosayebi, A. Ahmadzadeh, W. Wicke, V. Jamali, R. Schober, and M. Nasiri-Kenari, "Early cancer detection in blood vessels using mobile nanosensors," *IEEE Trans. on NanoBio.*, vol. 18, pp. 103–116, Apr. 2019.

[19] M. Turan, M. Kuran, H. B. Yilmaz, I. Demirkol, and T. Tugcu, "Channel model of molecular communication via diffusion in a vessel-like environment considering a partially covering receiver," in *Proc. 2018 IEEE Int. Black Sea Conf. on Commun. and Network. (BlackSeaCom)*, pp. 1–5, Jun. 2018.

[20] M. Schafer, W. Wicke, R. Rabenstein, and R. Schober, "Analytical models for particle diffusion and flow in a horizontal cylinder with

a vertical force," in *Proc. 2019 IEEE Int. Conf. on Commun. (ICC)*, pp. 1–7, May 2019.

[21] M. Turan, B. C. Akdeniz, M. Kuran, H. B. Yilmaz, I. Demirkol, A. E. Pusane, and T. Tugcu, "Transmitter localization in vessel-like diffusive channels using ring-shaped molecular receivers," *IEEE Commun. Lett.*, vol. 22, pp. 2511–2514, Dec. 2018.

[22] L. Felicetti, M. Femminella, and G. Reali, "Simulation of molecular signaling in blood vessels: Software design and application to atherogenesis," *Nano Commun. Net.*, vol. 4, pp. 98 – 119, Sep. 2013.

[23] W. Wicke, T. Schwering, A. Ahmadzadeh, V. Jamali, A. Noel, and R. Schober, "Modeling duct flow for molecular communication," in *Proc. 2018 IEEE Global Commun. Conf. (GLOBECOM)*, pp. 206–212, Dec. 2018.

[24] N. Farsad, D. Pan, and A. Goldsmith, "A novel experimental platform for in-vessel multi-chemical molecular communications," in *Proc. 2017 IEEE Global Commun. Conf. (GLOBECOM)*, pp. 1–6, Dec. 2017.

[25] N. Tavakkoli, P. Azmi, and N. Mokari, "Performance evaluation and optimal detection of relay-assisted diffusion-based molecular communication with drift," *IEEE Trans. on NanoBio.*, vol. 16, pp. 34–42, Jan. 2017.

[26] X. Wang, M. D. Higgins, and M. S. Leeson, "Relay analysis in molecular communications with time-dependent concentration," *IEEE Commun. Lett.*, vol. 19, pp. 1977–1980, Nov. 2015.

[27] Y. Moritani, S. Hiyama, and T. Suda, "Molecular communication among nanomachines using vesicles," in *Proc. of NSTI nanotech. conf.*, vol. 2, pp. 705–708, 2006.

[28] T. Soong, *Fundamentals of Probability and Statistics for Engineers*. Wiley, May 2004.

[29] Y. Fang, A. Noel, N. Yang, A. W. Eckford, and R. A. Kennedy, "Convex optimization of distributed cooperative detection in multi-receiver molecular communication," *IEEE Trans. on Mol. , Bio. and Multi-Scale Commun.*, vol. 3, pp. 166–182, Sep. 2017.

[30] S. Nallagonda, Y. R. Kumar, and P. Shilpa, "Analysis of hard-decision and soft-data fusion schemes for cooperative spectrum sensing in rayleigh fading channel," in *Proc. 2017 IEEE 7th Int. Adv. Comput. Conf. (IACC)*, pp. 220–225, Jan. 2017.

[31] S. Maleki, S. P. Chepuri, and G. Leus, "Optimization of hard fusion based spectrum sensing for energy-constrained cognitive radio networks," *Phy. Commun.*, vol. 9, pp. 193 – 198, Dec. 2013.

[32] Y. Fang, A. Noel, N. Yang, A. W. Eckford, and R. A. Kennedy, "Distributed cooperative detection for multi-receiver molecular communication," in *Proc. 2016 IEEE Global Commun. Conf. (GLOBECOM)*, pp. 1–7, Dec. 2016.

[33] A. Bensky, *Short-range Wireless Communication*. Elsevier Science, 3rd ed., 2019.

[34] B. Rapp, *Microfluidics: Modeling, Mechanics and Mathematics*. Micro and Nano Technologies, Elsevier Science, 2017.

[35] W. Wicke, T. Schwering, A. Ahmadzadeh, V. Jamali, A. Noel, and R. Schober, "Modeling duct flow for molecular communication," in *2018 IEEE Global Commun. Conf. (GLOBECOM)*, pp. 206–212, Dec 2018.

[36] G. I. Taylor, "Dispersion of soluble matter in solvent flowing slowly through a tube," *Proceedings of the Royal Society of London. Series A. Mathematical and Physical Sciences*, vol. 219, no. 1137, pp. 186–203, 1953.